Analyst

ROYAL SOCIETY OF CHEMISTRY

PAPER

View Article Online
View Journal | View Issue

Cite this: *Analyst*, 2020, **145**, 4512

An efficient assay for identification and quantitative evaluation of potential polysialyltransferase inhibitors†

Xiaoxiao Guo, Jodie R. Malcolm, Marrwa M. Ali, Goreti Ribeiro Morais, Steven D. Shnyder, Paul M. Loadman, Laurence H. Patterson and Robert A. Falconer *

The polysialyltransferases (polySTs) catalyse the polymerisation of polysialic acid, which plays an important role in tumour metastasis. While assays are available to assess polyST enzyme activity, there is no methodology available specifically optimised for identification and quantitative evaluation of potential polyST inhibitors. The development of an HPLC-fluorescence-based enzyme assay described within includes a comprehensive investigation of assay conditions, including evaluation of metal ion composition, enzyme, substrate and acceptor concentrations, temperature, pH, and tolerance to DMSO, followed by validation using known polyST inhibitors. Thorough analysis of each of the assay components provided a set of optimised conditions. Under these optimised conditions, the experimentally observed K_i value for CMP, a competitive polyST inhibitor, was strongly correlated with the predicted K_i value, based on the classical Cheng–Prusoff equation [average fold error (AFE) = 1.043]. These results indicate that this assay can provide medium-throughput analysis for enzyme inhibitors with high accuracy, through determining the corresponding IC_{50} values with substrate concentration at the K_M, without the need to perform extensive kinetic studies for each compound. In conclusion, an *in vitro* cell-free assay for accurate assessment of polyST inhibition is described. The utility of the assay for routine identification of potential polyST inhibitors is demonstrated, allowing quantitative measurement of inhibition to be achieved, and exemplified through assessment of full competitive inhibition. Given the considerable and growing interest in the polySTs as important anti-metastatic targets in cancer drug discovery, this is a vital tool to enable preclinical identification and evaluation of novel polyST inhibitors.

Received 10th April 2020,
Accepted 7th May 2020

DOI: 10.1039/d0an00721h

rsc.li/analyst

1. Introduction

Polysialyltransferases (polySTs), specifically enzymes ST8SiaII and ST8SiaIV, catalyse the biosynthesis of polysialic acid (polySia), which is a unique carbohydrate homopolymer of *N*-acetylneuraminic acid (sialic acid, Neu5Ac), linked specifically by α-2,8 glycosidic bonds. PolySia is found on several proteins in humans, but is predominantly observed as a post-translational modification of the neural cell adhesion molecule (NCAM). Whilst polySTs are active embryologically, with roles including driving the polySia-dependent migration of cells of neural crest origin in the foetus, polySia expression is generally dramatically reduced post-partum,[1,2] with relatively low level polySia expression only detectable in discrete areas of the brain, and in blood, milk, semen, and on immune cells.[2–7] Crucially, significant polySia expression is observed in many cancers, principally those of neuroendocrine origin, where the expression of polySTs is re-capitulated and is associated with tumour cell migration, invasion, and the events associated with metastasis. This is closely correlated with poor prognosis in the clinic.[8–14] The polySTs, and ST8SiaII in particular (generally thought to be the dominant enzyme in tumours where polySia is expressed[8,15]), have significant potential as drug targets in a number of difficult-to-treat cancers, notably neuroblastoma and small cell lung cancer.[8,16]

A number of *in vitro* assays have been developed and reported for the evaluation of polyST enzyme activity, utilising the enzyme, the substrate CMP-sialic acid, and the acceptor NCAM.[17–19] The Gerardy-Schahn group recently reported the utility of a non-ganglioside fluorescent acceptor, DMB-DP3, as a convenient substitute for NCAM, enabling analysis of polymerisation. DMB-DP3 is a trimer (degree of polymerisation,

Institute of Cancer Therapeutics, Faculty of Life Sciences, University of Bradford, Bradford BD7 1DP, UK. E-mail: r.a.falconer1@bradford.ac.uk; Tel: +44 (0)1274 235842

†Electronic supplementary information (ESI) available. See DOI: 10.1039/d0an00721h

DP = 3) of α-2,8-linked sialic acid ('DP3') derivatised with a fluorescent 1,2-diamino-4,5-methylenedioxybenzene (DMB) label thereby forming 'DMB-DP3'. This was successfully employed to assess bacterial and murine ST8SiaII enzyme activity.[18] Building on this work, we previously utilised DMB-DP3 to determine the activity of human polySTs, monitoring polymerisation of DMB-DP3 to predominantly DMB-DP4 (Fig. 1).[20] The fluorescent acceptor and product in the enzyme reaction are separated by reversed-phase chromatography over a short timeframe (10 min), while being simultaneously visualised by fluorescence detection (Fig. 1, inset), allowing rapid analysis. Whilst adequate for measurement of enzyme activity, this assay lacks the characteristics to deduce accurate kinetics required for detailed analysis of potential enzyme inhibitors.

In our research focused on the identification of novel polyST inhibitors, we require a reproducible medium-throughput quantitative assay for determination of enzyme inhibition, with the key additional requirement for robust detailed enzyme kinetics information, and compound mode of inhibition (*i.e.* competitive or non-competitive).[20,21] Herein we report a cell-free polyST assay that meets these demands. We have systematically investigated the assay parameters that are predicated to influence the underlying enzyme catalysis with a view to providing a sound basis on which to reliably determine mode of inhibition, IC_{50} and K_i values for putative inhibitors, the latter through both prediction and experiment. The optimised assay conditions were validated by evaluating known polyST small molecule inhibitors.

2. Materials and methods

2.1 Reagents

The following materials were obtained from Sigma-Aldrich, UK: cytidine-5′-monophospho-*N*-acetylneuraminic acid sodium salt (CMP-Sia, C8271), 4,5-methylenedioxy-1,2-phenylenediamine dihydrochloride (DMB, D4784), anhydrous magnesium chloride ($MgCl_2$, M8266), manganese chloride ($MnCl_2$, 8054), potassium chloride (KCl, P9333), sodium cacodylate trihydrate (C4945), glycerol solution (G5516), ammonium formate (AmF, F-2004), β-mercaptoethanol (M-7522), dimethyl sulfoxide (DMSO, D8418), trifluoroacetic acid: (98% Reagent Grade, T6508) and sodium hydrosulfite (157951).

N-Acetylneuraminic acid trimer DP3 (α,2–8) was purchased from Nacalai Tesque, Japan (00641-52). Human ST8SiaII recombinant protein was purchased from R&D systems (6590-GT, USA). Tris-base was purchased from Fisher Bioreagents UK (BP152-1). Sodium hydroxide was obtained from Alfa Aesar (A16037). The reversed-phase chromatography column (RPB, 2.1 × 250 mm, 5 μm particle size) was purchased from Hichrom Ltd, UK.

2.2 DMB-DP3 synthesis and purification

DMB-DP3 synthesis was conducted as described previously.[20] Briefly, DP3 (10 mg ml^{-1}) was dissolved in a labelling solution containing DMB (20 mM), sodium hydrosulfite (40 mM) and β-mercaptoethanol (1 M). The mixture was then added to an equal volume of ice-cold trifluoroacetic acid (40 mM), followed by incubation at 4 °C overnight. The reaction was subsequently

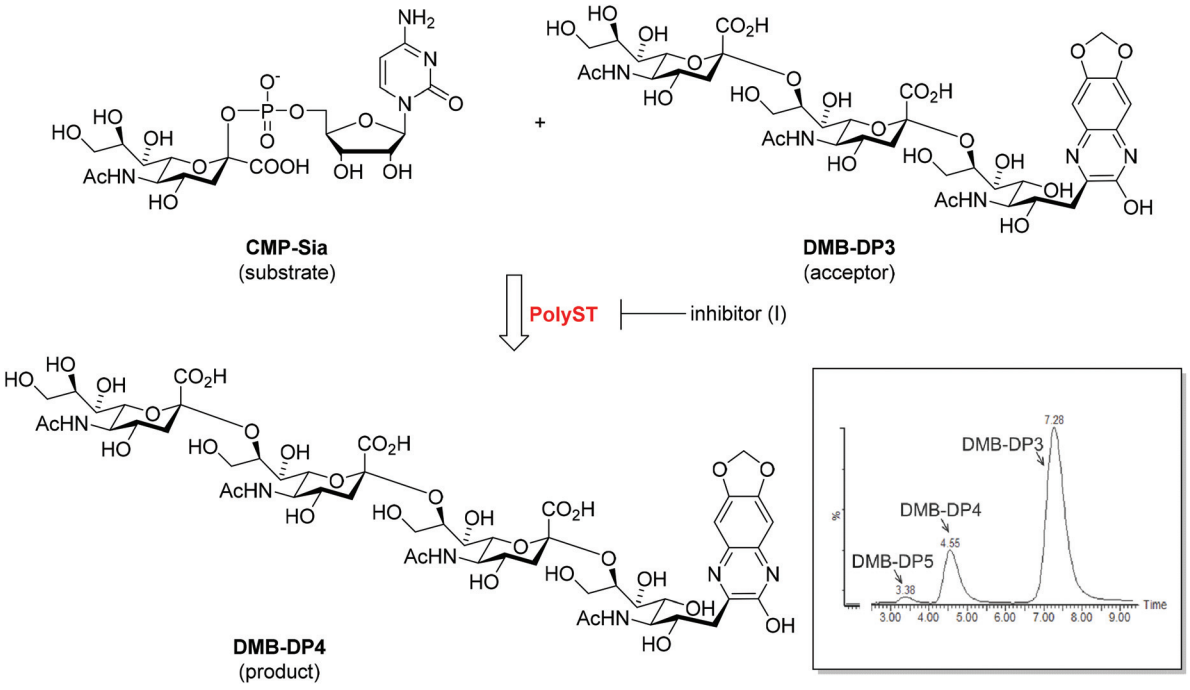

Fig. 1 The polysialyltransferase (polyST) enzyme reaction and analysis by HPLC; the enzyme reaction, polymerisation of DMB-DP3 (acceptor, as a substitute for NCAM) to DMB-DP4/DMB-DP5 catalysed by polyST, utilising CMP-Sia as substrate; [inset] an extract from a reversed-phase HPLC fluorescence chromatogram showing the DMB-DP3 acceptor, and DMB-DP4 and DMB-DP5 products from the enzyme reaction.

quenched by addition of one fifth of the reaction volume of sodium hydroxide (0.2 M). The synthesised DMB-DP3 was subsequently purified on a reversed-phase liquid chromatography-fluorescence detection system, as previously described.[20]

2.3 Enzyme assay characterisation

The initial polyST enzyme assay conditions were as described previously for the assessment of enzyme activity,[20] with minor modifications. Specifically, recombinant polyST (ST8SiaII) protein (250 ng) and DMB-DP3 (50 μM) were added to a solution containing $MgCl_2$ (20 mM), $MnCl_2$ (10 mM), 5% glycerol, and sodium cacodylate (10 mM, pH 6.7, adjusted by addition of HCl). The reaction was initiated by addition of the substrate, CMP-Sia (500 μM), and maintained at 25 °C for 2 h. The final reaction volume was 10 μl. The enzyme reaction was quenched by addition of 9 volumes of a stopping buffer containing Tris-HCl (100 mM, pH 8.0) and EDTA (20 mM), followed by incubation at 50 °C for 10 min. A 90% methanol precipitation step was then performed to remove the recombinant proteins prior to HPLC-fluorescence analysis, using centrifugation at 14 000 rpm (20 000*g*).

2.3.1 Effect of metal ions. Enzyme reactions containing sodium cacodylate buffer (10 mM, pH 6.7), DMB-DP3 (50 μM) and polyST protein (250 ng) were incubated with either Mg^{2+}, Mn^{2+} or K^+ ions, in concentrations ranging from 1–100 mM, as indicated in Fig. 2. Reactions were initiated by adding CMP-Sia (100 μM), and were carried out at 25 °C for 2 h as described above. The residual enzymatic activities were measured to evaluate the effects of metal ions on enzymatic activity.

2.3.2 Effect of incubation temperature. Analysis of enzyme kinetic parameters was carried out at a range of temperatures (10 °C, 15 °C, 20 °C, 25 °C, 30 °C, and 37 °C). In brief, enzyme reactions were incubated in the presence of the metal ion composition identified as optimal, while the remaining assay components were as described above, at each temperature of interest at pre-determined time points (0.5 h, 1 h, 2 h, 3 h, and 5 h). The initial velocities were evaluated to determine the catalytically optimum temperature.

2.3.3 Effect of incubation pH. Enzyme kinetics were characterised in a pre-designated pH environment containing various substrate concentrations. In brief, enzyme reactions were performed in buffer containing the previously determined optimal metal ion composition, cacodylate (10 mM) at a pH ranging from 4.90 to 7.20, and CMP-Sia (10–1000 μM), at 25 °C for pre-determined time points (0.5 h, 1 h, 2 h, 3 h, and 5 h). The initial velocities were evaluated to determine the optimum pH and the corresponding K_M values of substrate (CMP-Sia).

2.3.4 Effect of enzyme concentration. Kinetic parameters for polyST (5–100 ng μL^{-1}) were analysed by performing the enzyme assay in buffer containing the optimal metal ion composition, and temperature identified from the above, in the presence of CMP-Sia (500 μM) and DMB-DP3 (200 μM). Reactions were carried out for each enzyme concentration of interest at pre-determined time points (0.5 h, 1 h, 2 h, 3 h, and 4.5 h), in both the optimal and original pH environments. To avoid saturation of fluorescence detection, samples were diluted at least 10-fold.

2.3.5 Analysis of the K_M of acceptor (DMB-DP3). Subsequently, the apparent affinity constant (K_M) of DMB-DP3 for polyST was determined by carrying out the enzymatic reactions under the optimal conditions, in the presence of DMB-DP3 at various concentrations (10–300 μM). The corresponding initial velocities were determined.

2.3.6 Effect of DMSO. This was carried out by incubating enzymatic reactions in the optimised buffer containing CMP-Sia (24 μM) and polyST (250 ng) at pH 5.8 (the optimised pH determined above), in the presence of DMSO at various concentrations (0%, 1%, 2%, 5%) at 25 °C, at pre-determined time points (0.5 h, 1 h, 2 h, 3 h, and 5 h). The initial velocities were determined to evaluate DMSO tolerance.

2.4 HPLC-fluorescence analysis of polyST catalytic activity

PolyST enzymatic activity was determined by analysis of the conversion of DMB-DP3 to DMB-DP4 (and DMB-DP5, which is often additionally detected), using a reversed-phase HPLC system in conjunction with fluorescence detection. Samples for analysis were subjected to separation with a reversed-phase chromatographic column (2.1 × 250 mm, 5 μm, RPB-Hichrom, UK) eluting with methanol (16% in HPLC grade water) and ammonium formate (5 mM) using an isocratic mobile phase (350 μl min^{-1}) at 20 °C. Each chromatographic separation was conducted over 10 min. The DMB-labelled acceptor (DMB-DP3) and products (DMB-DP4 & DMB-DP5) were visualised using a fluorescence detector (Ex 373 nm/Em 448 nm (ref. 20)). The acquired chromatograms were analysed by Masslynx and Quanlynx software (Waters, UK).

2.5 Assessment relative potencies (IC_{50} values) for polyST inhibitors

For determination of IC_{50} values for known polyST inhibitors (CMP, and 5-methyl-CMP), enzymatic reactions were carried

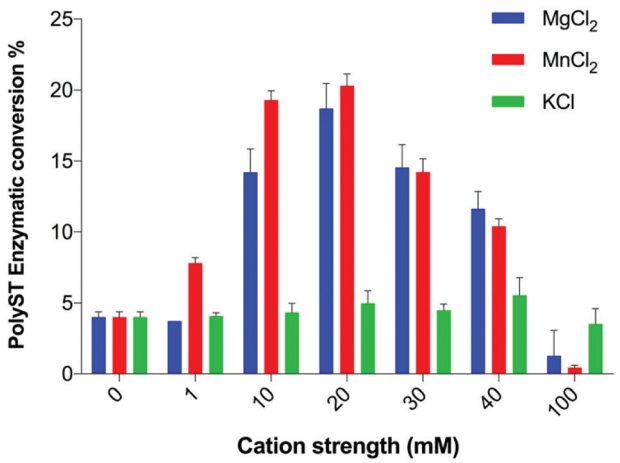

Fig. 2 Effects of individual metal ions on polyST enzymatic activity. Data plotted are mean values ± SD from 3 independent experiments.

out in the presence of each compound at pre-determined concentrations for 2 h. Enzyme reactions were carried out in the presence of 24 μM substrate (CMP-Sia), which is the K_M at the optimised conditions (see below). Experiments were performed in triplicate.

2.6 Assessment of inhibitory constant (K_i) for CMP

In order to determine inhibitory constant (K_i) for the known polyST inhibitor CMP, enzymatic reactions were performed in the presence of the inhibitor at each single concentration, with increasing concentrations of CMP-Sia substrate (0.5–5 K_M) at 25 °C at selected time points (specifically, 0.5, 1, 2, 3, and 5 h). Experiments were performed in triplicate.

2.7 Kinetics data analysis

PolyST enzymatic conversion of fluorescent acceptor (DMB-DP3) to fluorescent products (DMB-DP4 and DMB-DP5) was calculated from fluorescence signal peak areas (measured as Relative Fluorescence Units, RFU) of products and acceptor molecules, according to eqn (1):

$$\%\,\text{PolyST enzymatic conversion} = \text{RFU(Products)}/[\text{RFU(Products)} + \text{RFU(Acceptor)}] \quad (1)$$

Enzymatic transfer of Sia from substrate (CMP-Sia) to fluorescent acceptor was calculated from the percentage concentration of transferred Sia against total substrate concentration, according to eqn (2):

$$\%\,\text{Conversion[CMP-Sia]} = \%\,\text{Enzymatic conversion} \times [\text{Acceptor}]/[\text{Substrate}] \quad (2)$$

Percent enzyme inhibition was calculated using the % conversion values, based on eqn (1), obtained in the presence and absence of inhibitor according to the eqn (3):

$$\%\ \text{Inhibition} = [1 - \text{Conversion}\ (i)/\text{Conversion}\ (C)] \times 100\% \quad (3)$$

Inhibitor compound potency (IC_{50} value) was determined by plotting percentage inhibition as a function of inhibitor concentration and fitting in a normalised dose–response non-linear regression curve, using Graphpad Prism 6 software.

Initial velocities (v_0) for enzymatic reactions were calculated using differential equations derived from the respective enzyme reaction progress curves, using a time point of 0.01 h. The enzyme kinetics parameters were calculated by plotting initial reaction velocities [v_0] *versus* substrate concentration [S] and fitting the data points by non-linear regression to the classical Michaelis–Menten steady-state model:

$$V_0 = V_{max}^{(app)} \times [S]/([S] + K_M^{(app)}) \quad (4)$$

where v_0 is the initial reaction velocity (pmol min^{-1}), [S] represents the substrate concentration (μM), $V_{max}^{(app)}$ is the apparent maximum reaction velocity (pmol min^{-1}) and $K_M^{(app)}$ is the apparent Michaelis constant (μM).

The catalytic constant for the enzyme was estimated by the eqn (5), assuming a molecular mass of 41 kDa per subunit of ST8SiaII:

$$k_{cat} = V_{max}/[E_{Total}] \quad (5)$$

where k_{cat} is the catalytic constant (min^{-1}), V_{max} is the maximum reaction velocities (μM min^{-1}) and [E_{Total}] is the total enzyme concentration (μM).

The accuracy of the prediction for experimentally-measured intrinsic potency (K_i) values from half apparent potencies ($IC_{50}/2$) was determined by calculating the average fold error (AFE) according to eqn (6).[22]

$$\text{AFE} = 10\ \exp\ [1/n\ \sum \log(\text{Predicted}\ K_i/\text{measured}\ K_i)] \quad (6)$$

This methodology is based on absolute values of the logarithm of the ratio of predicted to measured values, so that negative values are also converted to positive values. An AFE value of 1 represents an ideal prediction.[22]

All data points presented are representative of 3 independent experiments, each with a minimum of 2 technical replicates.

3. Results and discussion

3.1 Assay development

Measuring the effect of small molecules on the cell-free catalytic activity of polyST is an effective way to identify novel inhibitors of this enzyme. Existing assays reported in the literature have focused on maximising enzyme activity, rather than providing the optimum conditions to measure enzyme inhibition, or to derive important information about mode of inhibition and kinetics data. We have thus undertaken an exploration of the reaction conditions, and have arrived at an assay with highly effective capability for inhibitor detection, including determination of K_i values and mode of inhibition. Given that ST8SiaII is the predominant of the two polySTs in cancer, this enzyme was the focus for these studies.

3.1.1 Metal ion composition. Previously published assays for polyST activity have reported methodologies that include varying combinations and concentrations of magnesium (Mg^{2+}), manganese (Mn^{2+}), potassium (K^+), and indeed calcium (Ca^{2+}) ions.[20,21,23–28] While Kitazume-Kawaguchi most recently suggested that metal ions are not required for human polyST enzyme activity,[23] Kojima had earlier provided evidence that activity was enhanced by both Mg^{2+} and Mn^{2+} ions at 10 mM, in the case of recombinant polyST enzymes,[24,25] albeit utilising NCAM as acceptor in each case.

We observed that polyST was significantly more active in the presence of Mn^{2+} than Mg^{2+} up to a concentration of 20 mM (Fig. 2). Higher concentrations of either ion led to a reduction in enzyme activity, as measured by conversion of acceptor DMB-DP3 to products DMB-DP4/DMB-DP5. This is in agreement with previous studies suggesting that Mn^{2+} was more important for human polyST activities than Mg^{2+}.[24,26,29]

K^+ ions exhibited very little effect on enzyme activity, while Mn^{2+} and Mg^{2+} ions significantly improved enzymatic activity (as compared to the control) up to a concentration of 40 mM, above which activity was reduced. Both divalent cations significantly improved enzyme activity at 20 mM. Furthermore, we demonstrated that the effects were not additive (Fig. S1†). The optimum metal ion composition in the enzyme assay buffer was thus selected as 20 mM $MnCl_2$, in the absence of $MgCl_2$ and KCl.

3.1.2 Effect of incubation temperature on enzyme activity. The effect of temperature on human polyST was investigated, by analysing enzyme reaction velocities at selected temperatures between 10 °C and 37 °C (Fig. 3). Results demonstrated a peak activity between 20–25 °C. Similarly to observations reported in previous studies,[20,30] 25 °C was identified as the optimum temperature for polyST kinetics over longer incubation periods, whereas reaction velocities were significantly reduced at 10 °C, and most interestingly at 37 °C. Moreover, the enzyme also maintained a high initial velocity at 20 °C, with relatively moderate enzyme activity between 15 °C and 30 °C. The metal ion composition determined in section 3.1.1 was utilised here.

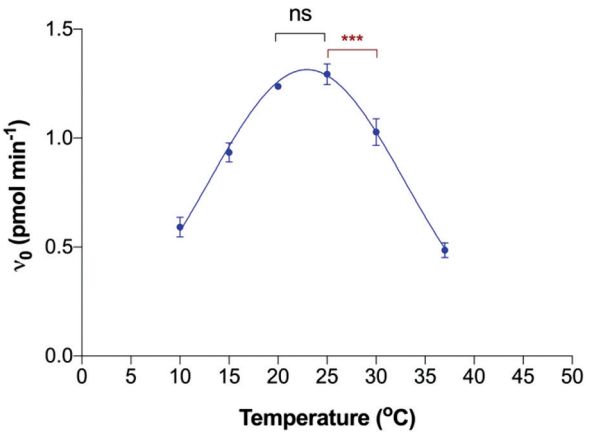

Fig. 3 Effect of temperature on polyST enzyme activity. Data plotted are mean values ± SD from 3 independent experiments. ***P < 0.0001; ns = not significant.

3.1.3 Effect of pH and substrate concentration. The activity of polyST was examined over a range of pH values (4.90–7.20) in cacodylate buffer. The optimum pH for a given enzyme reaction can vary with substrate concentration,[31] and the buffer pH has an influence on the K_M of substrate,[32] which in turn can affect the apparent potency (IC_{50} values) of enzyme inhibitors. With this in mind, we determined the influence of pH on polyST kinetic parameters, and enzyme reactions were performed at a range of substrate concentrations (10–1000 μM), and at 50 μM and 150 μM acceptor (DMB-DP3). Initial velocities were calculated from corresponding enzyme reaction progress curves (section 2.7), and were plotted against substrate concentration. Data were fit using a non-linear regression curve, according to the Michaelis–Menten model (Fig. 4A).

The corresponding kinetic parameters, V_{max}, k_{cat}, substrate (CMP-Sia) K_M and catalytic efficiency (k_{cat}/K_M) of polyST for CMP-Sia, measured at both acceptor concentrations, are summarised in Table 1. The results indicate that pH 5.8 was optimal for catalytic activity, at both low and high concentrations of the acceptor. This indicates that the effect of pH on the catalytic efficiency of polyST is independent of the acceptor concentration. The catalytic efficiencies, measured at 150 μM DMB-DP3, were then plotted against pH (Fig. 4B). These results are consistent with previously reported findings for the activity of human and chick brain polySTs for NCAM polysialylation with CMP-Sia, albeit in MES buffer and utilising NCAM as acceptor.[23,26,29] It is interesting that the enzyme activity is apparently optimal in slightly acidic conditions. A potential explanation for this phenomenon may be due to the pH in the Golgi apparatus in malignant cells (where this enzyme is

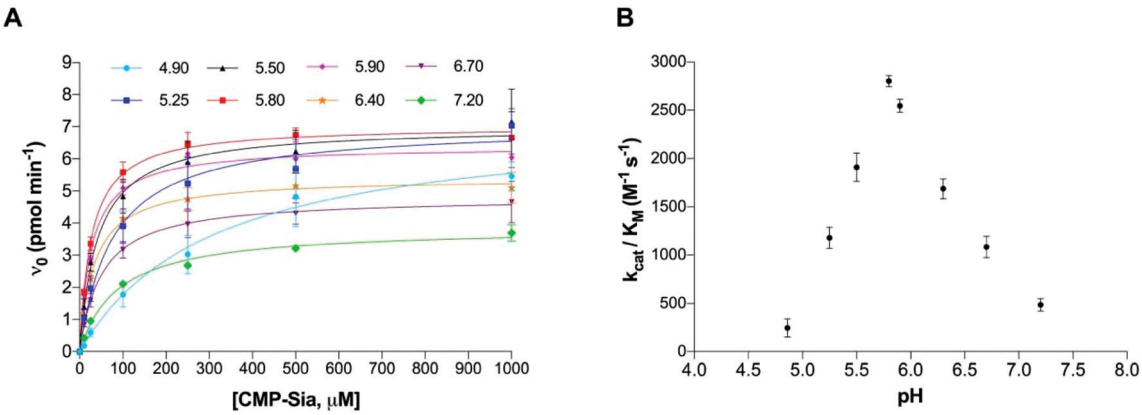

Fig. 4 Effect of substrate (CMP-Sia) concentration and pH on enzyme activity. (A) Initial velocities (v_0) of enzyme reactions in pH range 4.90–7.20 were plotted as a function of substrate (CMP-Sia) concentration, measured at an acceptor (DMB-DP3) concentration of 150 μM. The plot is a non-linear regression analysis to the Michaelis–Menten model. Data plotted are mean values ± SD from 3 independent experiments. (B) Effect of pH on catalytic efficiencies (k_{cat}/K_M) at an acceptor concentration of 150 μM. Reactions were carried out at 25 °C, using 20 mM $MnCl_2$.

Table 1 Kinetic parameters for the polyST enzyme reaction at 25 °C as a function of pH (utilising initial assay conditions outlined in section 2.3; app = apparent)

	50 μM DMB-DP3				150 μM DMB-DP3			
pH	$V_{max}^{(app)}$ (pmol min^{-1} μg^{-1})	k_{cat} (s^{-1})	$K_M^{(app)}$ (μM)	k_{cat}/K_M (s^{-1} M^{-1})	$V_{max}^{(app)}$ (pmol min^{-1} μg^{-1})	k_{cat} (s^{-1})	$K_M^{(app)}$ (μM)	k_{cat}/K_M (s^{-1} M^{-1})
5.25	10.41 ± 0.26	7.11×10^{-3}	52.39 ± 6.32	135.73	28.82 ± 0.58	0.079	67.32 ± 5.91	1170.31
5.5	9.17 ± 0.19	6.27×10^{-3}	34.54 ± 3.39	181.41	27.45 ± 0.84	0.075	39.16 ± 5.71	1916.11
5.8	7.65 ± 0.29	5.23×10^{-3}	23.64 ± 5.08	220.95	28.10 ± 0.48	0.077	26.88 ± 2.33	2857.78
6.7	5.57 ± 0.34	3.81×10^{-3}	57.29 ± 15.46	66.45	19.20 ± 0.58	0.052	50.34 ± 6.85	1042.50
7.2	3.78 ± 0.36	2.59×10^{-3}	92.35 ± 30.16	27.98	15.42 ± 0.42	0.042	86.98 ± 9.33	484.44

usually located) being mildly acidic at pH 5.8–6.2.[33,34] The optimum pH for the assay was thus selected as 5.8.

3.1.4 Effect of enzyme concentration. The effect of polyST enzyme concentration in the assay was investigated to ensure steady-state conditions prevailed during the course of the enzyme reaction, *i.e.* that a constant (linear) initial velocity was maintained throughout the reaction course. This requires, generally, that no more than 15% substrate depletion is observed at the end-point of an enzyme assay.[35] Furthermore, it is also preferable to keep the enzyme concentration as low as possible, so as to avoid a high 'IC_{50} wall' for putative tight-binding inhibitors.[36] The optimal enzyme concentration for the assay was determined by investigating the relationship between enzyme concentration and reaction velocity at saturated concentrations of substrate and acceptor (Fig. 5A), and measuring the corresponding CMP-Sia conversion (indirectly from DMB-DP3 to DMB-DP4/DMB-DP5 conversion, as described above) at a series of enzyme concentrations (Fig. 5B). Assays were performed under the optimal conditions for ion strength, temperature and pH described above.

To ensure the final enzyme concentration fell within the range that provides enzyme reaction linearity, the effect of enzyme concentration on the reaction velocity was analysed, and is shown in Fig. 5A. As expected, initial velocity increased linearly with increased enzyme concentration within the measured range of 5 to 100 ng μL^{-1}, with saturated concentrations of both substrate (500 μM) and acceptor (200 μM). This indicates that the assay is reliable for quantitative studies using enzyme concentrations within this range. Next, the corresponding donor substrate (CMP-Sia) conversion was analysed at each time point (Fig. 5B). At our routine screening time point (2 h), substrate conversion was approximately 15%, when the enzyme concentration was 25 ng μL^{-1}, while the conversion was lower than 10% when the enzyme concentration was lower than 15 ng μL^{-1}, in the presence of the saturated concentrations of CMP-Sia (500 μM) (Fig. 5B). Moreover, the donor substrate conversion at its original K_M (100 μM, pH 6.7) was also analysed at various enzyme concentrations (Fig. S2†). Enzyme conversion significantly reduced to approximately 8% in the presence of 25 ng μL^{-1} enzyme, and to lower than 3% when using enzyme concentrations lower than 15 ng μL^{-1} (Fig. S2†). The low conversion observed at lower enzyme concentrations (5–15 ng μL^{-1}) resulted in insufficient fluorescent signal (from the DMB-DP4 product) for reliable detection. In contrast, a substrate conversion of higher than 15%/2 h may not be favourable since the greater substrate depletion will not provide the ideal steady-state conditions previously discussed.[35,36] With these factors in mind, an enzyme concentration of 25 ng μL^{-1} (providing a substrate conversion of 8% at the 2 h screening time point) was thus selected for the optimised assay, with the concentration of CMP-Sia at its K_M.

3.1.5 Characteristics of kinetic parameters (K_M) for DMB-DP3. We subsequently measured the kinetic parameters for the acceptor, DMB-DP3, in the presence of 500 μM

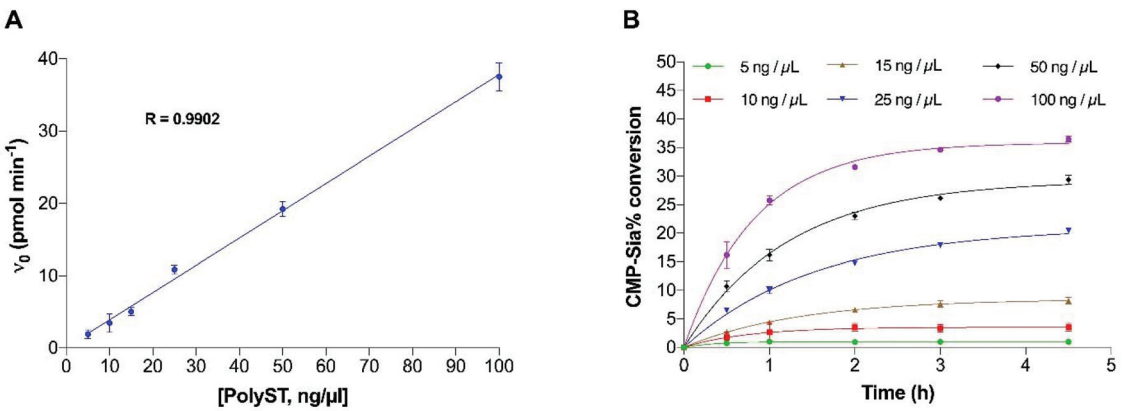

Fig. 5 Effect of polyST concentration on reaction initial velocity (A) and conversion of CMP-Sia (B), in the presence of 500 μM CMP-Sia. Data plotted are mean values ± SD from 3 independent experiments.

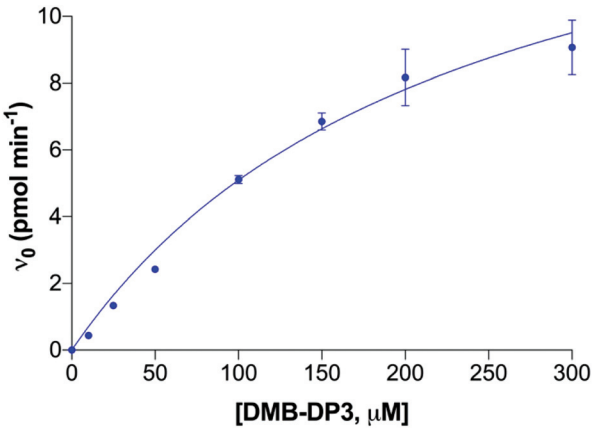

Fig. 6 A Michaelis–Menten plot of polyST initial velocity *versus* DMB-DP3 (acceptor) concentration. Data plotted are mean values ± SD from 3 independent experiments.

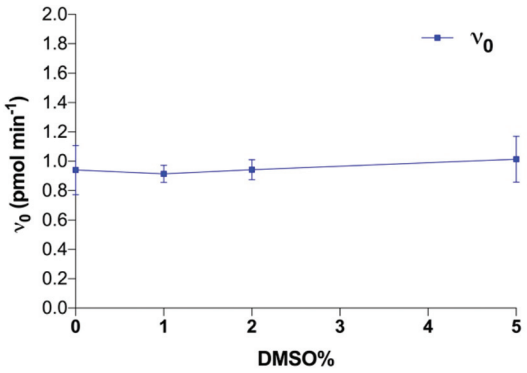

Fig. 7 Effect of DMSO on enzyme reaction velocity.

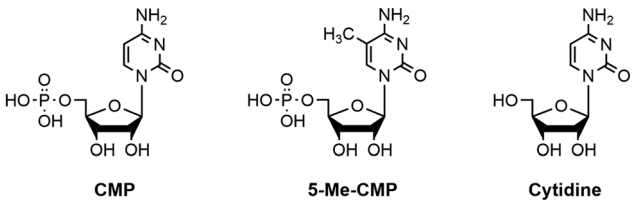

Fig. 8 Structures of cytidine monophosphate (CMP), 5-methyl-cytidine monophosphate (5-Me-CMP) and cytidine.

CMP-Sia substrate, to allow sufficient substrate conversion (Fig. 6). The apparent K_M of DMB-DP3 was approximately 230 μM in the optimised assay conditions (pH 5.8), according to the Michaelis–Menten model. Ideally, keeping the acceptor at a saturated concentration will favour the screening of compounds that are designed to compete with the substrate (*i.e.* CMP-Sia). The DMB-DP3 acceptor concentration had no significant effect on the binding affinity of the donor substrate, however (see section 3.1.3). Given the fluorescent signal for DMB-DP3 at 100 μM could exceed the linearity range without further dilution (Fig. S3†), the final concentration of DMB-DP3 was fixed at 50 μM.

3.1.6 Determination of polyST tolerance to DMSO. Limited aqueous solubility is a common challenge associated with screening for early hits in inhibitor discovery and DMSO is frequently added to aid solubility and to facilitate preparation of compound stock solutions. Effects on enzyme kinetics were evaluated in the assay conditions of $MnCl_2$ (20 mM), at pH 5.8 and 25 °C, over a range of DMSO concentrations (0–5%). The reaction was initialised by adding substrate (CMP-Sia, 24 μM = K_M). A concentration of DMSO up to 5% did not influence the enzyme reaction velocity (Fig. 7). A DMSO concentration of 5% was thus selected (as sufficient to aid compound solubility).

3.2 Assay validation using known polyST inhibitors

In order to test if the assay conditions are suitable for determination of IC_{50}, mode of inhibition and K_i of potential polyST inhibitors, we next explored the effect of known compounds CMP and 5-methyl-CMP (5-Me-CMP).[37] CMP and 5-Me-CMP have both been previously reported as inhibitors of polyST (in addition to other sialyltransferases).[38] Cytidine was also evaluated as a negative control, *i.e.* a compound known to have no effect on polyST catalytic activity (structures shown in Fig. 8).

The inhibitory potency of CMP is shown in Fig. 9A. The inhibitory (IC_{50}) dose–response curves shifting to the right with increasing concentrations of substrate (CMP-Sia), in the optimised assay conditions, is consistent with competitive inhibition. Enzyme kinetic parameters for CMP were thereby evaluated (Fig. 9B). In the classical Dixon plot (Fig. 9C), lines intersected in the second quadrant. In the Cornish-Bowden plot (Fig. S4†), the parallel lines and higher y-intercept ($[S]/V_0$) values with increased substrate concentration are consistent with competitive inhibition.[39] Taken together, these data provide further evidence for the competitive mode of inhibition for CMP.

To further evaluate the reliability of the assay in determining the potency of enzyme inhibitors, the intrinsic potency (K_i) of CMP was also determined from the Dixon plot, using the new assay conditions (Fig. 9C and Table 2). Subsequently, the ratio of the IC_{50} over the observed K_i was plotted as a function of the ratio of the substrate over K_M. The ratio of IC_{50}/K_i of CMP increased with increasing substrate concentration (Fig. 9D), demonstrating that CMP competed with the substrate in the optimised assay conditions. Furthermore, we also confirmed that CMP does not compete with the acceptor DMB-DP3 (Fig. S5†).

IC_{50} is not a direct indicator of enzyme binding affinity, although the two can be related for competitive inhibitors by the Cheng–Prusoff equation.[40] According to the Cheng–Prusoff theory for competitive inhibition, the substrate concentration has distinct effects on the apparent potency (IC_{50}) of inhibitors of different classes. When the substrate concentration is lower than its K_M, it favours the screening and identification of competitive inhibitors, and disfavours screening uncompetitive inhibitors, which only bind to substrate-bound

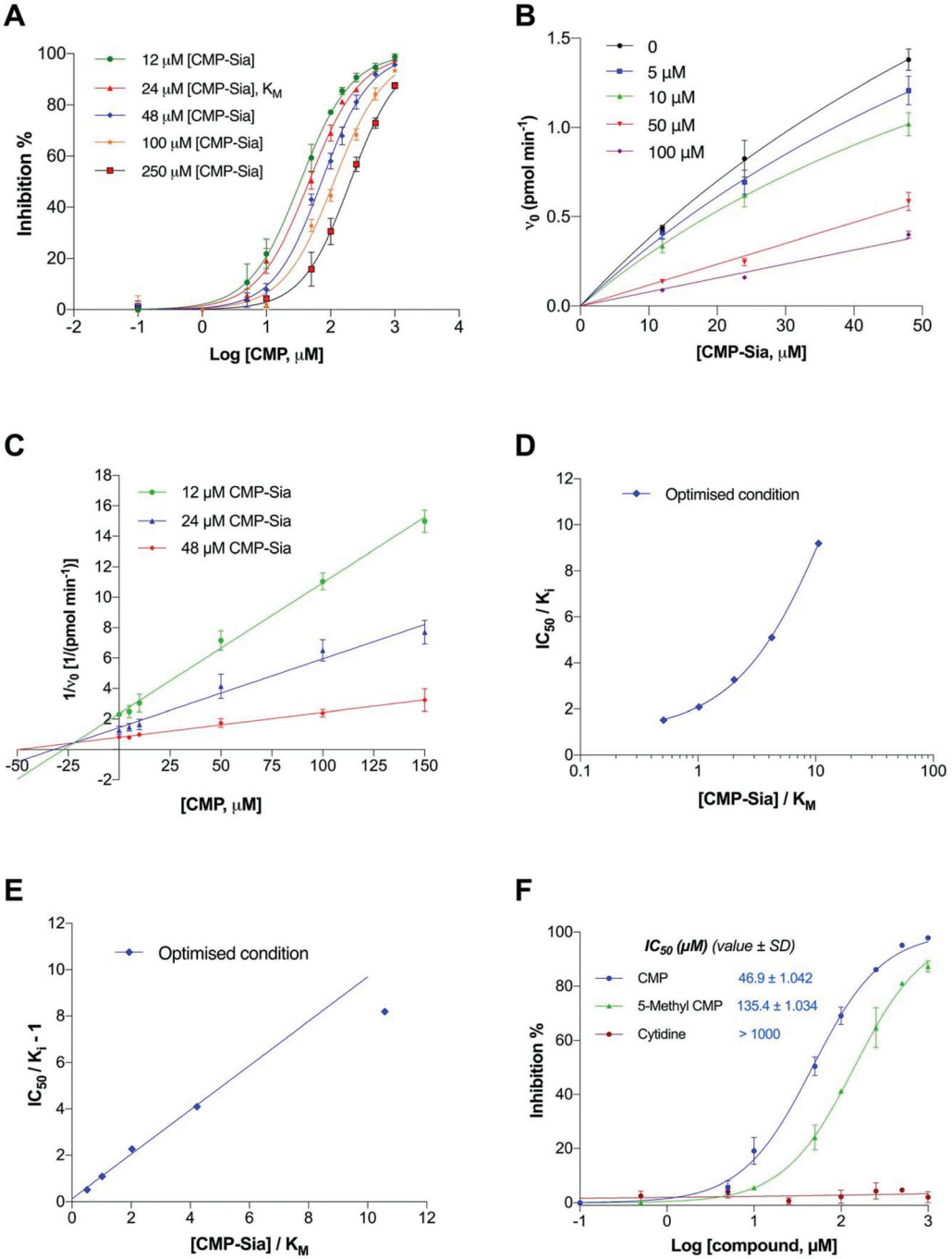

Fig. 9 Assay validation by determining the enzyme inhibitory potency and mode of inhibition of CMP. (A) Concentration-dependent inhibition of polyST by CMP in the presence of various substrate concentrations; (B) Michaelis–Menten plot of initial velocities for polyST in the presence of various inhibitor (CMP) concentrations; (C) Dixon plot for the data presented in B, for analysis of intrinsic potency (K_i) of CMP; (D) and (E) changes in apparent potencies (IC_{50} values) of CMP as a function of substrate concentration in a semi-log plot (D) and in a linear plot (E); (F) IC_{50} curves for CMP and 5-Me-CMP in optimised assay conditions ([S] = K_M). Data plotted are mean values ± SD from 3 independent experiments.

Table 2 Summary of measured apparent potencies (IC_{50}) and intrinsic potencies (K_i) for CMP

	CMP IC_{50} (μM)				K_M (CMP-Sia, μM)	Predicted K_i (μM)	Observed K_i (μM)	AFE (K_i)
CMP-Sia (μM)	12	24	48	100				
	$0.5K_M$	K_M	$2K_M$	$4K_M$				
Optimised assay	33.76	46.16	72.45	112.9	23.64 ± 5.08	22.91 ± 0.521	22.12 ± 0.216	1.043

enzymes, whereas the substrate concentration has no effect on changing the apparent potency (IC_{50}) for non-competitive inhibitors.[40–42]

The IC_{50} values of competitive inhibitors are close to their K_i values when the substrate concentration is significantly lower than the K_M, while the IC_{50} values of uncompetitive inhibitors only reflect their K_i values when the substrate concentration is significantly higher than the K_M. In contrast, the IC_{50} values of non-competitive inhibitors are independent from the concentration of enzyme substrates.[40,43] Therefore, in general, to identify enzyme inhibitors from all modalities, the most appropriate substrate concentration is at the K_M, which allows for balanced assay conditions, with minimum bias towards any of these important inhibitor classes.[42]

To directly determine if the relationship between measured IC_{50} and K_i for CMP fits well in the Cheng–Prusoff equation ($IC_{50}/K_i = 1 + [S]/K_M$), values of ($IC_{50}/K_i - 1$) were plotted linearly against the ratios of $[S]/K_M$, as shown in Fig. 9E. It is clear that the graph generated from the optimised assay conditions fits better to the Cheng–Prusoff equation, when the substrate concentration is five times lower than its K_M, than that obtained from the initial assay conditions (Fig. S6†).

In addition, according to Cheng–Prusoff, the K_i value for a competitive inhibitor should ideally be 50% of the IC_{50} value in a given assay, when the substrate concentration equal to the K_M. Therefore, using $IC_{50}/2$, the predicted K_i value is reported alongside the observed K_i for CMP in Table 2. The observed K_i value correlates well to the predicted value [$IC_{50}/2([S] = K_M)$] in the optimised assay (average fold error, AFE = 1.043), when substrate concentrations are in the range of $(0.5–4)K_M$, indicating feasibility for utilising IC_{50} values generated within these substrate concentrations for predicting K_i of CMP.

We next investigated assay sensitivity in terms of being able to distinguish compounds with potentially similar potencies, by determining the IC_{50} value of a CMP analogue (5-Me-CMP), in comparison to CMP. Cytidine was used as control.

As shown in Fig. 9F, CMP exhibited slightly higher enzymatic inhibition than 5-Me-CMP in the optimised assay, and these results are clearly distinguishable. These relative potencies are in agreement with findings reported for inhibition of polysialylation of the neural cell adhesion molecule (NCAM) catalysed by recombinant human polyST enzymes *in vitro*, albeit in an assay based on ^{14}C-labelled sialic acid incorporation into polySia, and subsequent SDS-PAGE of the polymer produced.[37] The negative control, cytidine, had no inhibitory effects even at 1 mM (as expected).

In summary, these data demonstrate the opportunity to predict intrinsic potencies (K_i) with confidence from the corresponding apparent potency values (IC_{50}) at the K_M, avoiding the need for extensive kinetic experiments normally required for such analysis.

3.2.1 Summary of optimised polyST assay conditions. Recombinant polyST (ST8SiaII) protein (250 ng) and DMB-DP3 (50 μM) were added to an aqueous solution containing $MnCl_2$ (20 mM), and sodium cacodylate (10 mM, pH 5.8, adjusted by addition of HCl). The reaction was initiated by addition of substrate, CMP-Sia (24 μM), and maintained at 25 °C for 2 h. The final reaction volume was 10 μl. The enzyme reaction was subsequently quenched by addition of 9 volumes of a stopping buffer containing Tris-HCl (100 mM, pH 8.0) and EDTA (20 mM), followed by incubation at 50 °C for 10 min. A 90% methanol precipitation step was then performed to remove the recombinant proteins prior to HPLC-fluorescent analysis, using centrifugation at 14 000 rpm (20 000*g*).

4. Conclusions

We report a sensitive, accurate, reproducible and robust enzyme assay for screening novel polyST enzyme inhibitors that has been optimised through a comprehensive assay development process. The optimised assay conditions allow quantitative measurements of polyST activity and compound inhibition, and the usefulness of the assay has been demonstrated in assessment of full competitive inhibition. These assay conditions additionally provide for the ability to confidently estimate K_i values from IC_{50} values for enzyme inhibitors. Given the significant interest in the polyST enzymes as important anti-metastatic targets in cancer drug discovery, this is a vital tool to enable identification and quantitative evaluation of novel polyST inhibitors, and to gain early insight into mode of inhibition. This work represents an essential step towards ultimately developing a novel clinically-useful therapeutic.

Author contributions

Conceived and designed the experiments: XG & RAF. Performed the experiments: XG, JRM, MMA & GRM. Data analysis: XG, JRM, MMA, & GRM. Supervisory team: SDS, PML, RAF. Manuscript composition and editing: XG, LHP & RAF. Final proof-reading: All.

Conflicts of interest

There are no conflicts to declare.

Acknowledgements

Ms Amanda Race is thanked for HPLC technical expertise. This work was funded by Yorkshire Cancer Research (LHP, RAF) and the Wellcome Trust (RAF).

References

1 J. L. Bruses and U. Rutishauser, *Biochimie*, 2001, **83**, 635–643.
2 J. Finne, *J. Biol. Chem.*, 1982, **257**, 11966–11970.
3 K. Angata, J. Nakayama, B. Fredette, K. Chong, B. Ranscht and M. Fukuda, *J. Biol. Chem.*, 1997, **272**, 7182–7190.

4 K. Zlatina, M. Saftenberger, A. Kuhnle, C. E. Galuska, U. Gartner, A. Rebl, M. Oster, A. Vernunft and S. P. Galuska, *Int. J. Mol. Sci.*, 2018, **19**, 1679.
5 U. Yabe, C. Sato, T. Matsuda and K. Kitajima, *J. Biol. Chem.*, 2003, **278**, 13875–13880.
6 P. Simon, S. Baumner, O. Busch, R. Rohrich, M. Kaese, P. Richterich, A. Wehrend, K. Muller, R. Gerardy-Schahn, M. Muhlenhoff, H. Geyer, R. Geyer, R. Middendorff and S. P. Galuska, *J. Biol. Chem.*, 2013, **288**, 18825–18833.
7 C. Ulm, M. Saffarzadeh, P. Mahavadi, S. Muller, G. Prem, F. Saboor, P. Simon, R. Middendorff, H. Geyer, I. Henneke, N. Bayer, S. Rinne, T. Lutteke, E. Bottcher-Friebertshauser, R. Gerardy-Schahn, D. Schwarzer, M. Muhlenhoff, K. T. Preissner, A. Gunther, R. Geyer and S. P. Galuska, *Cell. Mol. Life Sci.*, 2013, **70**, 3695–3708.
8 R. A. Falconer, R. J. Errington, S. D. Shnyder, P. J. Smith and L. H. Patterson, *Curr. Cancer Drug Targets*, 2012, **12**, 925–939.
9 M. Suzuki, M. Suzuki, J. Nakayama, A. Suzuki, K. Angata, S. Chen, K. Sakai, K. Hagihara, Y. Yamaguchi and M. Fukuda, *Glycobiology*, 2005, **15**, 887–894.
10 U. Valentiner, M. Muhlenhoff, U. Lehmann, H. Hildebrandt and U. Schumacher, *Int. J. Oncol.*, 2011, **39**, 417–424.
11 S. C. Schreiber, K. Giehl, C. Kastilan, C. Hasel, M. Muhlenhoff, G. Adler, D. Wedlich and A. Menke, *Gastroenterology*, 2008, **134**, 1555–1566.
12 S. M. Elkashef, S. J. Allison, M. Sadiq, H. A. Basheer, G. Ribeiro Morais, P. M. Loadman, K. Pors and R. A. Falconer, *Sci. Rep.*, 2016, **6**, 33026.
13 L. Gong, X. Zhou, J. Yang, Y. Jiang and H. Yang, *Oncol. Rep.*, 2017, **37**, 131–138.
14 F. Tanaka, Y. Otake, T. Nakagawa, Y. Kawano, R. Miyahara, M. Li, K. Yanagihara, J. Nakayama, I. Fujimoto, K. Ikenaka and H. Wada, *Cancer Res.*, 2000, **60**, 3072–3080.
15 K. Bork, D. Gagiannis, A. Orthmann, W. Weidemann, M. Kontou, W. Reutter and R. Horstkorte, *J. Neurochem.*, 2007, **103**(Suppl. 1), 65–71.
16 X. Guo, S. M. Elkashef, P. M. Loadman, L. H. Patterson and R. A. Falconer, *Carbohydr. Polym.*, 2019, **224**, 115145.
17 S. Inoue, S. L. Lin, Y. C. Lee and Y. Inoue, *Glycobiology*, 2001, **11**, 759–767.
18 T. G. Keys, F. Freiberger, J. Ehrit, J. Krueger, K. Eggers, F. F. Buettner and R. Gerardy-Schahn, *Anal. Biochem.*, 2012, **427**, 107–115.
19 J. Ehrit, T. G. Keys, M. Sutherland, S. Wolf, C. Meier, R. A. Falconer and R. Gerardy-Schahn, *ChemBioChem*, 2017, **18**, 1332–1337.
20 S. M. Elkashef, M. Sutherland, L. H. Patterson, P. M. Loadman and R. A. Falconer, *Analyst*, 2016, **141**, 5849–5856.
21 Y. M. Al-Saraireh, M. Sutherland, B. R. Springett, F. Freiberger, G. Ribeiro Morais, P. M. Loadman, R. J. Errington, P. J. Smith, M. Fukuda, R. Gerardy-Schahn, L. H. Patterson, S. D. Shnyder and R. A. Falconer, *PLoS One*, 2013, **8**, e73366.
22 L. J. Haupt, F. Kazmi, B. W. Ogilvie, D. B. Buckley, B. D. Smith, S. Leatherman, B. Paris, O. Parkinson and A. Parkinson, *Drug Metab. Dispos.*, 2015, **43**, 1744–1750.
23 S. Kitazume-Kawaguchi, S. Kabata and M. Arita, *J. Biol. Chem.*, 2001, **276**, 15696–15703.
24 N. Kojima, M. Kono, Y. Yoshida, Y. Tachida, M. Nakafuku and S. Tsuji, *J. Biol. Chem.*, 1996, **271**, 22058–22062.
25 N. Kojima, Y. Tachida, Y. Yoshida and S. Tsuji, *J. Biol. Chem.*, 1996, **271**, 19457–19463.
26 M. B. Sevigny, J. Ye, S. Kitazume-Kawaguchi and F. A. Troy 2nd, *Glycobiology*, 1998, **8**, 857–867.
27 J. Cheng, H. Yu, K. Lau, S. Huang, H. A. Chokhawala, Y. Li, V. K. Tiwari and X. Chen, *Glycobiology*, 2008, **18**, 686–697.
28 D. Nakata, L. Zhang and F. A. Troy 2nd, *Glycoconjugate J.*, 2006, **23**, 423–436.
29 S. Oka, J. L. Bruses, R. W. Nelson and U. Rutishauser, *J. Biol. Chem.*, 1995, **270**, 19357–19363.
30 T. Lindhout, C. R. Bainbridge, W. J. Costain, M. Gilbert and W. W. Wakarchuk, *PLoS One*, 2013, **8**, e69888.
31 M. H. Ross, J. O. Ely and J. G. Archer, *J. Biol. Chem.*, 1951, **192**, 561–568.
32 V. Sancenon, W. H. Goh, A. Sundaram, K. S. Er, N. Johal, S. Mukhina, G. Carr and S. Dhakshinamoorthy, *Biomol. Detect. Quantif.*, 2015, **4**, 1–9.
33 A. Rivinoja, F. M. Pujol, A. Hassinen and S. Kellokumpu, *Ann. Med.*, 2012, **44**, 542–554.
34 A. Rivinoja, N. Kokkonen, I. Kellokumpu and S. Kellokumpu, *J. Cell Physiol.*, 2006, **208**, 167–174.
35 G. Wu, Y. Yuan and C. N. Hodge, *J. Biomol. Screening*, 2003, **8**, 694–700.
36 R. A. Copeland, *Methods Biochem. Anal.*, 2005, **46**, 1–265.
37 T. Miyazaki, K. Angata, P. H. Seeberger, O. Hindsgaul and M. Fukuda, *Glycobiology*, 2008, **18**, 187–194.
38 L. Wang, Y. Liu, L. Wu and X. L. Sun, *Biochim. Biophys. Acta*, 2016, **1864**, 143–153.
39 A. Cornish-Bowden, *Biochem. J.*, 1974, **137**, 143–144.
40 Y. Cheng and W. H. Prusoff, *Biochem. Pharmacol.*, 1973, **22**, 3099–3108.
41 M. G. Acker and D. S. Auld, *Perspect. Sci.*, 2014, **1**, 56–73.
42 J. Yang, R. A. Copeland and Z. Lai, *J. Biomol. Screening*, 2009, **14**, 111–120.
43 R. A. Copeland, *Anal. Biochem.*, 2003, **320**, 1–12.